

1 **Soil organic matter build-up during soil formation in glacier forelands**

2 **around the world**

3 Khedim Norine ^{1,2}, Cécillon Lauric ^{3,4}, Poulenard Jérôme ¹, Barré Pierre ⁴, Baudin François ⁵, Marta
4 Silvio ⁶, Rabatel Antoine ⁷, Dentant Cédric ¹³, Cauvy-Fraunié Sophie ⁹, Anthelme Fabien ¹², Gielly
5 Ludovic ², Ambrosini Roberto ⁶, Franzetti Andrea ⁸, Azzoni Roberto Sergio ⁶, Caccianniga Marco
6 Stefano ¹⁴, Compostella Chiara ¹⁵, Clague John ¹⁶, Tielidze Levan ^{10,11}, Messenger Erwan ¹, Choler
7 Philippe ², Ficetola Francesco ^{2,6}

8

9 ¹ Univ. Savoie Mont-Blanc, Univ. Grenoble Alpes, CNRS, EDYTEM, F-73000 Chambéry, France

10 ² Univ. Grenoble Alpes, Univ. Savoie Mont-Blanc, CNRS, LECA, F-38000 Grenoble, France

11 ³ Univ. Normandie, UNIROUEN, INRAE, ECODIV, F-76000 Rouen, France

12 ⁴ Univ. PSL, Laboratoire de Géologie, CNRS-ENS UMR 8538, Ecole Normale Supérieure, Paris,

13 France

14 ⁵ Univ. Sorbonne, CNRS, UMR ISTeP, Paris, France

15 ⁶ Univ. of Milan, Department of Environmental Science and Policy, I-20126 Milan, Italy

16 ⁷ Univ. Grenoble Alpes, CNRS, IRD, Institut des Géosciences de l'Environnement UMR 5001, F-

17 38000 Grenoble, France

18 ⁸ Univ. of Milano Bicocca, Department of Earth and Environmental Science, I-20126 Milan, Italy

19 ⁹ INRAE, UR RIVERLY, Centre de Lyon-Villeurbanne, Villeurbanne Cedex, France

20 ¹⁰ Antarctic Research Centre, Victoria University of Wellington, P.O. Box 600, 6140, Wellington,
21 New Zealand

22 ¹¹ School of Geography, Environment and Earth Sciences, Victoria University of Wellington, P.O.
23 Box 600, 6140, Wellington, New Zealand

24 ¹² Univ. de Montpellier, AMAP, IRD, CIRAD, CNRS, INRA, Montpellier, France

25 ¹³ Parc national des Écrins, Domaine de Charance, Gap, France

26 ¹⁴ Univ. of Milan, Department of Biosciences, Via Celoria 26, I-20133 Milano, Italy

27 ¹⁵ Univ. of Milan, Department of Earth Sciences 'A. Desio', Milano, Italy

28 ¹⁶ Simon Fraser University, Department of Earth Sciences, 8888 University Drive, Burnaby, BC
29 V5A 1S6, Canada

30

31

32

33

34

35

36

37

Contact information: norine.khedim@univ-smb.fr; lauric.cecillon@inrae.fr

38 Abstract

39 Since the last glacial maximum, soil formation related to ice-cover shrinkage has been a major sink of
40 carbon accumulating as soil organic matter (SOM), a phenomenon accelerated by the ongoing global
41 warming. In recently deglaciated forelands, processes of soil organic matter accumulation, including
42 those that control carbon and nitrogen sequestration rates and biogeochemical stability of newly
43 sequestered carbon, remain poorly understood. Here, we investigate the build-up of SOM during the initial
44 stages of soil formation (up to 410 years) in ten glacier forelands distributed on four continents. We test
45 whether the net accumulation of SOM on glacier forelands (i) depends on the time since deglaciation
46 and climatic conditions (temperature and precipitation); (ii) is accompanied by a decrease in its stability;
47 (iii) is mostly due to an increasing contribution of organic matter from plant origin. We measured total
48 SOM concentration (C, N), its relative H/O enrichment, stable isotopic (^{13}C , ^{15}N) and carbon functional
49 groups (C-H, C=O, C=C) compositions, and the distribution in carbon pools of different thermal stability.
50 We show that SOM content increases with time and is faster on forelands experiencing warmer climates.
51 The build-up of SOM pools shows consistent trends across the studied chronosequences. During the first
52 decades of soil formation, the low amount of SOM is dominated by a thermally stable carbon pool with a
53 small and highly thermolabile pool. The stability of SOM decreases with soil age at all sites, reflecting plant
54 carbon inputs to soil (SOM depleted in N, enriched in H and in aromatic C) and indicating that SOM storage
55 is dominated by the accumulation of labile SOM during the first centuries of soil formation. Our findings
56 highlight the vulnerability of SOM stocks from proglacial areas to global warming and suggest that their
57 durability largely depends on the relative contribution of carbon inputs from plants.

58 **Keywords:** soil organic matter, carbon stability, chronosequence, climate sensitivity, soil formation

59 **Introduction**

60 Since the last glacial maximum (*ca.* 20 kyr), more than 10 % of the Earth's land surface area has been freed
61 from its ice cover (Adams & Faure, 1998). In 2010, the total glacierized area (*ca.* 200.000 glaciers excluding
62 the Greenland and Antarctic ice sheets) was estimated at 0.72 Mkm², but ongoing climate change is
63 accelerating glacier ice loss (Pfeffer et al., 2014). As an example, in the European Alps, 25–30 % of ice cover
64 disappeared over the past 60 years (Gardent et al., 2014; Smiraglia & Azzoni, 2015). Based on the RCP 8.5
65 scenario, mountain glaciers are expected to lose 37 to 57% of their mass by 2100, and many will disappear
66 regardless even at lower emission scenarios (Hock et al., 2019). This accelerating ice shrinkage will lead to
67 the rise of novel terrestrial ecosystems conditioned by biodiversity dynamics, landform changes and soil
68 development (Eichel et al., 2016).

69 Globally, soils are a major terrestrial reservoir of carbon (*e.g.* Jobbágy & Jackson, 2000). Soil development
70 has led to accumulation of significant amounts of carbon as organic matter in formerly glaciated areas (*e.g.*
71 Albrecht, 1938; Schlesinger, 1995). Despite high uncertainties, up to one-third (*i.e.* 490 GtC) of the current
72 global soil organic carbon (SOC) has been sequestered in soils since the Last Glacial Maximum (Adams et
73 al., 1990; Adams & Faure, 1998). The rate of postglacial carbon sequestration as soil organic matter (SOM)
74 strongly varies with time after barren substrate exposure. Net SOC accumulation rates are usually greatest
75 during the early stages of soil formation in proglacial areas, but also depend on climatic conditions
76 (Bockheim, Birkeland, & Bland, 2000; Egli et al., 2012; Harden et al., 1992; Schlesinger, 1990).

77 By modelling postglacial SOC sequestration, Harden et al. (1992) emphasized the strong sensitivity of their
78 simulations to SOC decomposition dynamics, while regretting the lack of knowledge on the relative
79 contributions of labile (*i.e.* fast-cycling) and stable (slow-cycling) SOC kinetic pools within soil
80 chronosequences. Accumulation of SOM in glacier foreland soils with low net primary production and low
81 rate of SOM degradation is also a key element of ecosystem development in the early stages of successions

82 (Schulz et al., 2013; Wietrzyk et al., 2018; Yoshitake et al., 2018). During the past 15 years, researchers
83 have examined the distribution of SOC in different kinetic pools as soils form in glacier forelands (*e.g.*
84 Bardgett et al., 2007; Egli et al., 2012; Schweizer et al., 2018), using chemical (*e.g.* Egli et al., 2012), physical
85 (*e.g.* Conen et al., 2007) or thermal (Bardgett et al., 2007) SOM fractionation methods, in some cases in
86 combination with elemental isotopic signatures of SOM (^{15}N , ^{13}C , ^{14}C ; Bardgett et al., 2007; Smittenberg et
87 al., 2012) or other SOM characterization techniques such as ^{13}C nuclear magnetic resonance or Fourier
88 transform mid-infrared spectroscopy (Dümig et al., 2012; Egli et al., 2010). The main assumptions from
89 these works are: (1) a stable and ancient SOC fraction – whose origin is still debated – may be the primary
90 source of carbon and energy for microbial communities during the first decades of soil formation (Bardgett
91 et al., 2007; Guelland et al., 2013), while nitrogen would mostly originate from atmospheric deposition
92 (Smittenberg et al., 2012); (2) organo-mineral associations evolve in early stages of soil development, with
93 SOC sequestration occurring at a faster rate than soil mineral weathering (Dümig et al., 2012; Schweizer
94 et al., 2018). However, discrepancies remain among studies regarding the evolution of SOC stability during
95 the formation of proglacial soils and the build-up of their SOM stocks. Indeed, Bardgett et al. (2007)
96 showed that SOC stability decreased during soil development, whereas Egli et al. (2010) showed that the
97 proportion of stable SOC increased and other researchers did not identify clear temporal changes in SOC
98 stability (Conen et al., 2007; Egli et al., 2012). Such inconsistencies may relate to local environmental
99 conditions. Moreover, the methods used for partitioning stable from labile SOC may also affect study
100 outcomes, as none of the currently available SOM fractionation methods can reliably isolate SOC fractions
101 that are unique and non-composite in terms of carbon turnover times in soil (von Lützow et al., 2007;
102 Smith et al., 2002). The same is true for thermal methods (*e.g.* Balesdent, 1996), which have, however,
103 demonstrated that biogeochemically stable SOC was thermally stable (Barré et al., 2016; Gregorich et al.,
104 2015; Plante et al., 2013; Sanderman & Grandy, 2020).

105 To date, most studies of the dynamics of SOM and the fate of SOC fractions in glacier forelands have
106 focused on one or a few glacier forelands within the same area. In addition, most studies have been
107 performed in the European Alps (*e.g.* Damma, Morteratsch and Ödenwinkelkees glaciers), the U.S. Rocky
108 Mountains (*e.g.* Wind River Range) and the high Arctic region (Ny-Ålesund) (*e.g.* Burga et al., 2010; Dümig
109 et al., 2012; Eckmeier et al., 2013; Egli et al., 2012; Nakatsubo et al., 2005; Schurig et al., 2013; Schweizer
110 et al., 2018), with very limited information from tropical areas and the Southern Hemisphere. As a result,
111 we are constrained in our ability to draw general conclusions about the drivers of net SOM accumulation
112 rates and the build-up of SOC kinetic pools in proglacial environments.

113 In this paper, we use a global dataset on SOM dynamics during the initial stage (*i.e.* up to 410 years) of soil
114 formation and ecosystem development in alpine proglacial areas. Specifically, we test three hypotheses:
115 (i) the accumulation of SOM in glacier forelands at the early stage of soil build-up is affected by time and
116 is accelerated by a warmer climate; (ii) irrespective of local conditions, there is a common pattern of
117 decreasing SOM stability along soil chronosequences in glacier forelands (*i.e.* SOM newly accumulated in
118 glacier forelands soils is mostly labile); and (iii) the accumulation of SOM in glacier forelands is mainly
119 driven by an increasing contribution of organic matter from plant origin. To test these hypotheses, we
120 examine the effect of climatic variables on the dynamics of SOM accumulation in soil chronosequences in
121 ten glacier forelands around the world and evaluate the qualitative evolution of newly accumulated SOM
122 over time by studying the thermal stability of carbon, the functional groups of organic carbon, the
123 elemental stoichiometry of SOM and the stable isotopes of nitrogen and carbon.

124 ***Material and methods***

125 **Study sites, soil sampling and climatic data**

126 This study is based on data from ten glacier forelands spread over four continents (Figure 1): Glaciers
127 Noir/Blanc (France), Forni (Italy), Gergeti (Georgia), Tiedemann (Canada), Charquini and Zongo (Bolivia),
128 Antisana (Ecuador), Perito Moreno (Argentina), Lobuche (Nepal), and Apusnikajik (Greenland). Study sites
129 encompass a wide range of geographic and climatic variables (*i.e.* latitude, elevation, mean annual
130 temperature and precipitation). Soil sampling was performed between October 2014 and July 2017. In
131 each glacier foreland, we sampled soil from three to eight dated plots to obtain a chronosequence of soil
132 development (see kmz file in Supplementary Informations). Well-dated chronosequences were
133 established using dendrochronological, lichenometric radiocarbon, optically stimulated luminescence
134 techniques, photogrammetry and time series reconstruction based on satellite images and old maps (Table
135 1). For each plot, five topsoil samples (0–15 cm; 15 g each) were collected at a distance of more than 20
136 m from one another and mixed together to form a composite sample. The short timescale studied (< 410
137 years after exposure of barren soil) and similar soil parent material at all sampling plots (Table 1) ensure
138 that the chronosequences are a suitable space-for-time substitution tool (Johnson & Miyanishi, 2008;
139 Walker et al., 2010).

140 For each glacier foreland, we extracted two climate variables from the CHELSA dataset (Climatologies at
141 High Resolution for the Earth's Land Surface Areas; Karger et al., 2017), with a resolution of 30 arc-seconds
142 (approximately 1 km at the equator) averaged over the period 1979-2013: mean air temperature of
143 warmest quarter (T, °C) and precipitation of warmest quarter temperature (P, mm month⁻¹). The CHELSA
144 dataset uses ERA-Interim reanalyzes to downscale climate surface variables accounting for topography
145 (Karger et al., 2017). Other global climate gridded datasets such as TerraClimate database (Abatzoglou et
146 al., 2018) yield similar results.

147 **Soil organic matter analysis**

148 Total soil C and N concentrations were measured in each composite soil sample by elemental analysis (OEA
149 Flash2000, ThermoFisher). As none of the foreland soils has a carbonate parent material, total soil C
150 concentration corresponds to the total SOC concentration. ^{13}C and ^{15}N content were measured by isotope
151 ratio mass spectrometry (ELEMENTAR Isoprime) and the results expressed in $\delta^{13}\text{C}$ and $\delta^{15}\text{N}$ abundance
152 ratios (*i.e.* in parts per thousand (‰) relative to international standards). These indexes provide
153 information about the origin of the SOM. In proglacial soils, high $\delta^{13}\text{C}$ values have been linked to the
154 presence of ancient carbon (Bardgett et al., 2007), although it also depends on the type of photosynthesis
155 of autotrophic organisms that are present. Persistent SOC has been shown to have higher $\delta^{13}\text{C}$ values in
156 comparison to bulk SOC (Balesdent & Mariotti, 1996; Brüggemann et al., 2011; Menichetti et al., 2015).
157 Negative $\delta^{15}\text{N}$ values are generally associated with biological nitrogen fixation or atmospheric nitrogen
158 deposition (Smittenberg et al., 2012).

159 The composition of organic carbon functional groups in topsoil samples was assessed by Fourier transform
160 mid-infrared spectroscopy (FTIR) in the attenuated total reflectance (ATR) mode. FTIR measurements were
161 performed using a Nicolet iS10 spectrometer (Thermo Fischer Scientific) equipped with a diamond crystal
162 ATR device. Finely ground samples were dried overnight (40°C) to standardize their water content prior to
163 analysis. FTIR spectra of bulk soil were acquired over the 4000–650 cm^{-1} spectral range, with a spectral
164 resolution of 4 cm^{-1} and 16 scans. Spectra were corrected for atmospheric interferences (H_2O and CO_2),
165 and absorbance values were calculated as the inverse logarithm of the measured reflectance values. FTIR
166 spectra were pre-processed (offset-correction using the 4000–3950 cm^{-1} spectral region as a reference,
167 and setting the minimum absorbance value to zero). Three FTIR waveband-regions were selected,
168 corresponding to specific organic carbon functional groups, and relatively free from artifact absorptions
169 by soil minerals in soils free of carbonates (adapted from Soucémarianadin et al., 2019): (1) the aliphatic
170 (CH_2, CH_3 stretch) waveband-region between 2930 and 2900 cm^{-1} ; (2) the carbonyl and carboxyl ($\text{C}=\text{O}$

171 stretch) waveband-region between 1750 and 1670 cm^{-1} ; (3) the aromatic carbon (C=C bond) waveband-
172 region between 1610 and 1590 cm^{-1} . Relative ratios for these three regions were then calculated (FTIR C-
173 H; FTIR C=O; FTIR C=C) using Eq. (1):

$$174 \text{ Relative ratio (region } i) = \frac{\text{area region } i}{(\sum(\text{area of 3 regions}))} \quad (1)$$

175 Areas of waveband-regions were divided by their respective spectral region width (30 cm^{-1} for C-H, 80 cm^{-1}
176 for C=O, 20 cm^{-1} for C=C) prior to the calculation of relative ratios.

177 The organic matter bulk chemistry and thermal stability was characterized by Rock-Eval® thermal analysis
178 using a Rock-Eval® 6 Turbo device (Vinci Technologies). This technique, which does not require any
179 chemical pre-treatment of the soil sample, involves the measurement of carbon as gaseous effluent during
180 two phases (Behar, Beaumont & De B. Penteadó, 2001; Cécillon et al., 2018; Disnar et al., 2003). The first
181 phase is a pyrolysis stage (200–650 °C) in a N_2 atmosphere, during which CO and CO_2 gases are quantified
182 with an infrared detector and volatile hydrocarbon effluents (CH) are quantified using a flame ionization
183 detector. The second phase is an oxidation stage (300–850 °C) in a laboratory air atmosphere, during which
184 CO and CO_2 gases are quantified with an infrared detector.

185 Using the combination of the five Rock-Eval® thermograms (Behar, Beaumont & De B. Penteadó, 2001),
186 we defined three SOC pools of different thermal stability (Figure S1): (i) a small and highly thermolabile
187 pyrolysable organic carbon pool (hereafter termed POC 1), corresponding to the carbon evacuated as CH,
188 CO or CO_2 at 200°C over three minutes during the pyrolysis phase; (ii) an intermediate pyrolysable organic
189 carbon pool (hereafter termed POC 2), corresponding to the carbon evacuated as CH, CO or CO_2 during
190 the temperature ramp-up (30°C min^{-1}) of the pyrolysis phase between 200 and 650°C; and (iii) a pool of
191 organic carbon resistant to pyrolysis (hereafter termed ROC), corresponding to the carbon evacuated
192 during the oxidation phase as CO or CO_2 . As is the case with all SOM fractionation methods, thermal
193 analysis does not isolate unique and non-composite SOC kinetic pools (von Lützow et al., 2007), yet SOC

194 thermal stability is positively correlated to SOC biogeochemical stability (Barré et al., 2016; Sanderman &
195 Grandy, 2020). Therefore, the Rock-Eval® thermal SOC fractions POC 1, POC 2 and ROC correspond to three
196 SOC fractions containing increasing proportions of biogeochemically stable SOC. The three Rock-Eval®
197 thermal SOC fractions are expressed as concentration (g C kg^{-1}) or as percentage of total SOC.

198 The thermal stability of the Rock-Eval® thermal SOC fractions that are pyrolyzable or resistant to pyrolysis
199 has been shown positively correlated to the proportion of persistent SOC (Cécillon et al., 2018). We thus
200 additionally determined the temperature corresponding to the release of 50% and 90% of the carbon from
201 the Rock-Eval® thermal SOC fractions POC 2 and ROC (*i.e.* T50-POC 2, T90-POC 2, T50-ROC, T90-ROC;
202 expressed in °C) in order to characterize more accurately the thermal stability of the carbon included in
203 these two RE thermal SOC fractions. Higher values of these indexes indicate higher thermal stability of the
204 considered thermal SOC fraction. For the two pyrolysable Rock-Eval® thermal SOC fractions (POC 1 and
205 POC 2), we also quantified the proportion of SOC carbon released as volatile hydrocarbon effluents (CH)
206 to estimate the SOM enrichment in hydrogen for POC 1 (CH-POC 1, unitless) and POC 2 fractions (CH-POC
207 2, unitless). These two indexes are negatively correlated to the oxygen content of SOM in the POC 1 and
208 POC 2 fractions.

209 Low SOC concentrations of topsoil samples from glacier forelands present a challenge to the quality of the
210 Rock-Eval® signals. Soil samples with a SOC concentration below 1 g C kg^{-1} were discarded, as we
211 considered those values below the detection limit of the Rock-Eval®6 Turbo device. Similarly, we discarded
212 soil samples with carbon yields below 75% and above 125% of the SOC concentration determined with
213 elemental analysis (EA). With these two constraints, we retained Rock-Eval® results for 37 topsoil samples,
214 representing eight glacier forelands (all Rock-Eval® results from soil samples of the Lobuche Glacier
215 foreland in the central Himalaya and the Charquini glacier foreland in the Central Andes were discarded).
216 The summary statistics of Rock-Eval® carbon yield (% of SOC elemental analysis) for the 37 retained topsoil
217 samples are as follows: mean = 96%; median = 94%; minimum = 77%; maximum = 124% (Table S3).

218 **Statistical analysis**

219 We used general mixed models to assess the factors related to the evolution of SOM characteristics in
220 glacier forelands (SOC, total N concentration, C and N stable isotope signatures ($\delta^{13}\text{C}$ and $\delta^{15}\text{N}$), organic
221 carbon functional groups (FTIR C-H, FTIR C=O, FTIR C=C), Rock-Eval[®] POC 1, POC 2, and ROC fractions (% of
222 total SOC and g C kg^{-1}), thermal stability of the Rock-Eval[®] POC 2 and ROC fractions (T50-POC 2, T90-POC
223 2, T50-ROC, T90-ROC), and the CH proportion of the Rock-Eval[®] POC 1 and POC 2 fractions (CH-POC 1 and
224 CH-POC 2)). Explanatory variables include time since barren substrate/debris exposure (soil age, year),
225 mean air temperature (T, °C) and precipitation (P, mm) of warmest quarter average over the period 1979-
226 2013. Because the effect of climate on SOM might change through time, we tested the relationship
227 between age and climatic parameters. Non-significant effects were removed from the final models. To
228 take into account the heterogeneity among glacier forelands, the identity of the foreland was included as
229 a random factor. In preliminary mixed models, we also tested a quadratic term (age^2) to verify the linearity
230 of the age/SOM relationship. Significant quadratic terms indicate that relationships between SOM and age
231 are non-linear. However, the quadratic term was not significant in any the models, indicating a lack of
232 significant deviation from the linear patterns. Therefore, in the final models we only retained the linear
233 relationship. For each dependent variable, we tested mixed models with both random intercept (RI) and
234 random slope (RS), and selected the one with lowest Akaike's Information Criterion (AIC; Burnham &
235 Anderson, 2002; Schielzeth & Forstmeier, 2009). The RI model assumes that the relationship between age
236 and SOM has the same slope, but different intercept across sites, whereas the RS model assumes a
237 difference in both intercept and slope across sites.

238 Additionally, we used mixed models to assess the evolution of SOM characteristics with SOC and total N
239 concentrations. Statistical analysis was performed with R v.3.5 (R Core Team, 2018) and the MuMIn and
240 lme4 libraries. Before running analyses, we log-transformed soil age, temperature, precipitation, SOC and
241 total N concentrations, the concentration of the different RE thermal SOC fractions, and T50 and T90 to

242 improve normality and reduce skewness. The CH-POC 1, CH-POC 2 indexes, the proportions of the different
243 RE thermal SOC fractions and the FTIR indexes were logit-transformed for the same reasons. The variables
244 C/N, $\delta^{15}\text{N}$, $\delta^{13}\text{C}$ were normally distributed.

For Review Only

245 **Results**

246 **Organic carbon, total nitrogen concentrations and C/N ratio of topsoils**

247 Soil organic carbon (SOC) concentrations are very low (generally $< 2 \text{ g C kg}^{-1}$) in all soils less than 25 years
248 old, but thereafter increased linearly with age without reaching a plateau (Figure 2a). Statistical analysis
249 of the relationship between soil age and temperature showed that the rate of SOC accumulation through
250 time is significantly different among glacier forelands, with faster SOC accumulation in forelands with the
251 warmest quarter of the year (Table 2). Furthermore, SOC concentration is directly related to the
252 temperature of the warmest quarter (Table 2). We found no significant relationship between SOC
253 concentration and precipitation of the warmest quarter of the year (Table 2).

254 Nitrogen concentration is very low on soils younger than 25 years - between 0.04 g N kg^{-1} and
255 0.46 g N kg^{-1} (Figure 2b). Nitrogen exceeded 1 g N kg^{-1} in topsoils about 50 years post deglaciation for
256 alpine chronosequences. The Zongo, Gergeti and Charquini forelands show soil nitrogen concentrations
257 above 1 g N kg^{-1} , respectively, 143, 150 and 260 years after deglaciation. Soil nitrogen concentration is
258 strongly related to soil age, but with a lower slope than for SOC concentration (Table 2). We did not detect
259 a significant slow-down in soil nitrogen over the first 410 years of soil development. Moreover, the rate of
260 soil nitrogen accumulation is significantly faster in forelands with warmer climates (Table 2).

261 The C/N ratio of topsoils is generally very low (< 5) at the earliest stage of soil formation, but increase with
262 soil age (Figure 2c). At Perito Moreno, Apusinkajik, Zongo and Charquini, the C/N ratio of topsoils reached
263 a plateau about 100 years after deglaciation, with values of about 10, whereas in the others forelands
264 the C/N rate continued to increase to 14–21 after 100 years (Tiedemann, Forni, Gergeti and Noir/Blanc).
265 However, the model that test the non-linear relationship between C/N and soil age was not significant (p
266 value = 0.69). Glacier forelands with warmer temperatures showed significantly higher soil C/N ratios and
267 a faster increase of soil C/N ratio with soil age than those with cooler temperatures (Table 2).

268 **Stable C and N isotopes and C functional groups in soil organic matter**

269 The $\delta^{13}\text{C}$ signature of SOM differs among the glacier forelands, especially in topsoils with low SOC
270 concentration (Figure 3a). Soil $\delta^{13}\text{C}$ is significantly lower in warmer forelands than cooler ones (Table 2).
271 We found no significant relationship between $\delta^{13}\text{C}$ and soil age (Table 2), but there is a significant negative
272 relationship between the $\delta^{13}\text{C}$ and SOC concentration (Figure 3a): soil $\delta^{13}\text{C}$ is higher on low-carbon soils
273 and decreases significantly as SOC increases (B value = -0.37, F value = -2.50, df = 52.20, p value = 0.016).

274 The $\delta^{15}\text{N}$ signature of SOM also differs considerably among the glacier forelands (Figure 3b), ranging from
275 -4‰ to $+4\text{‰}$ on average. Soils from the Gergeti, Noir/Blanc, Tiedemann, Forni and Apusinikajik forelands
276 have the lowest $\delta^{15}\text{N}$ values (around -4‰); those from the Charquini, Zongo, Perito Moreno, Lobuche and
277 Antisana forelands are greater than -2‰ . Soil $\delta^{15}\text{N}$ values increase significantly with soil age, and the
278 signature is lowest in forelands with warmer temperatures (Table 2). We also detect a weak positive
279 relationship between $\delta^{15}\text{N}$ values and the total concentration of nitrogen (B value = 0.42, F value = 1.76,
280 df = 52.33, p value = 0.08).

281 The FTIR signature of SOM changes with soil age and SOC concentration. The aromaticity (FTIR C=C) of
282 SOM increases significantly with soil age and SOC concentration, whereas the SOM content in aliphatic
283 carbon (FTIR C-H), carbonyl/carboxyl functional groups (FTIR C=O) decrease (Table 2, S2). SOM content in
284 aromatic carbon (FTIR C=C) is positively related to the temperature of the warmest quarter, and the
285 statistical analysis of the relationship between soil age and temperature showed that the rate of increase
286 in the aromatic carbon content of SOM through time is significantly different among glacier forelands, with
287 faster increase in SOM aromaticity in forelands with the warmest quarter of the year (Table 2).

288 **Soil organic carbon thermal stability**

289 Average Rock-Eval[®] thermal SOC fractions POC 1, POC 2 and ROC are, respectively, 0.1, 1.2 and
290 1.8 g C kg^{-1} between 9 and 50 years post deglaciation and, respectively, 0.1, 5.6 and 8.5 g C kg^{-1} between

291 150 to 220 years post deglaciation. The absolute amounts of all these pools increase significantly with
292 soil age and are highest in forelands with higher temperatures and precipitation (Table 2). POC 1, POC 2
293 and ROC thermal SOC fractions are 3.2%, 40.8% and 56.0% of total SOC, respectively, between 9 and 50
294 years post deglaciation and represented 1.3 %, 39.2 % and 59.5 %, respectively, 150 to 220 years post
295 deglaciation. The proportion of the POC 1 fraction significantly decreases with soil age, whereas the
296 contribution of the ROC fraction significantly increases with soil age (Table 2; Figures 4a,b). The proportion
297 of POC 1, which is the only fraction to be correlated with SOC concentration, decreases with SOC
298 accumulation (Table S2).

299 We detected a significant decrease in Rock-Eval® T50 and T90 indexes with soil age and with SOC
300 concentration, which indicates a general decrease in the thermal stability of the POC 2 and ROC fractions
301 (Tables 2, S2; Figures 4c,d). Furthermore, we found a significant decrease in the proportion of CH with soil
302 age and SOC in the POC 1. In contrast, we found that the proportion of CH in the POC 2 fraction increases
303 with soil age and SOC (Tables 2, S2; Figures 4e,f).

304 **Discussion**

305 In all the glacier forelands that we studied, the amount of organic matter in topsoils increased with time.
306 This SOM build-up is significantly modulated by climate: a warmer climate accelerates SOM accumulation.
307 Our second main finding is the common pattern of decreasing SOM stability along the chronosequences,
308 observed over all the glacier forelands studied. Then, with the observed changes in SOM elemental
309 stoichiometry, aromaticity and stable isotope signature with SOM accumulation, we see an increasing
310 contribution of organic matter from plant origin during the first centuries of soil formation.

311

312 **Temporal and climatic trends of organic matter accumulation in topsoils of glacier forelands**

313 Measured concentrations of soil organic carbon and total nitrogen in the ten glacier forelands are in good
314 agreement with previous observations. For example, similar SOC concentrations were reported for
315 topsoils in the Morteratsch glacier foreland in Switzerland (*i.e.* about 3 g C kg⁻¹ around 30 years; Eckmeier
316 et al., 2013), and similar very low nitrogen concentrations have been reported for the Zongo and Charquini
317 forelands in Andes (*i.e.* < 1 g N kg⁻¹ for soils under 80 years old; Schmidt et al., 2008). For all the glacier
318 forelands that we studied, time since exposure of the substrate was the major driver of the evolution of
319 the concentration in SOC and total N over the first 410 years of topsoil formation (Table 2). Some studies
320 analyzing the evolution of organic matter quantity in glacial foreland soils have shown a non-linear
321 relationship between C and N concentrations or stocks and soil age (*e.g.* Darmody, Allen & Thorn, 2005;
322 Harden et al., 1992), with a slowdown of organic matter accumulation after several hundred years (300-
323 700 years), and a plateau after several hundred or thousand years (Bockheim, Birkeland & Bland, 2000;
324 Dümig, Smittenberg & Kögel-Knabner, 2011; Egli, Fitze & Mirabella, 2001; Harden et al., 1992; He & Tang,
325 2008; Mavris et al., 2010). Our results show linear, non-saturating, SOC accumulation during the early
326 stages of the succession; the short time-scale of our study probably precluded the detection of later

327 slowdowns of SOM accumulation, but suggest a more regular pattern of organic matter accumulation
328 during the early stages (first 2-4 centuries) of establishment of the new ecosystem.

329 Contrary to previous reports (Göransson, Venterink & Bååth, 2011; Smittenberg et al., 2012), the C/N ratio
330 of SOM increases with soil age at all sites. This result suggest that SOC storage does not require N storage
331 equivalent to the initial C/N of SOM, as shown by Erktan (2013) in the early stage of soil chronosequences
332 formation in different ecosystems, with young topsoils starting at a similar C/N ratio of *ca.* 5–6. Therefore,
333 the low amount of N in topsoil is not a limiting factor for accumulation of SOM, nor probably for SOC
334 storage in the early stages of foreland soil formation.

335 In our study, temperature of the warmest quarter has a significant effect on SOM accumulation dynamics.
336 The relationship between SOM accumulation and climate in glacier forelands has previously been
337 observed and attributed to the effect of temperature and moisture (Bockheim et al., 2000; Egli et al., 2012).
338 To date, the lack of in situ measurements has hampered a more in-depth analysis of the local climate
339 drivers of SOM accumulation in glacier forelands. Even if global gridded datasets cannot adequately
340 capture these local climates, our findings provide evidence that temperature has a dominant role on SOM
341 accumulation in glacial forelands. This inference is consistent with results of studies of high-elevation
342 ecosystems, which show that primary productivity is primarily temperature-limited (Körner, 2003). Water
343 balance-related variables such as evapotranspiration or climatic water deficit do not have as strong an
344 effect on the primary productivity as the temperature of the warmest quarter. Further analyses should
345 investigate the interplay between temperature, precipitation and soil moisture on SOM accumulation,
346 preferably using locally observed values rather than global gridded data sets.

347 The effect of temperature during the warmest quarter on SOM accumulation can be explained by an
348 increase in SOM input. Notably, this positive effect is not offset by the increased heterotrophic activity and
349 SOM mineralization expected under a warmer climate. Thus continuous SOM accumulation with time in
350 the forelands indicates that the SOM input to soil is its key driver during the first centuries of soil formation.

351 Better quantification of SOM inputs along each chronosequence and across sites would be valuable in
352 refining our understanding of SOM accumulation. To overcome the difficulties of assembling field data at
353 the global scale, further studies should investigate the potential of using high-resolution remote sensing
354 to develop proxies of primary productivity in glacial forelands (Fischer et al., 2019). Finally, it is important
355 to note that we focused on SOM concentration in topsoils and that patterns could be different for SOM
356 stocks through the entire soil profile, especially in older soils with thicker, better developed profiles.

357

358 **Changes in SOC stability during soil formation and SOM accumulation**

359 Despite the diversity of climates, we detected consistent and general patterns in the build-up of SOC
360 fractions with different stability during soil formation and the associated accumulation of SOM (Figure 5).
361 First, the thermal stability of SOC decreased with soil age and with SOC concentration, as shown for the
362 POC 2 and the ROC fractions (representing *ca.* 97–99% of total SOC; Figures 4c, d and 5). This suggests that
363 the overall biogeochemical stability of SOC decreases as a soil ages and SOC sequesters in the soil; thus
364 the accumulation of SOC during the first centuries of soil formation in glacial forelands is preferentially
365 driven by the accumulation of labile SOC. The decrease in SOC biogeochemical stability with increasing
366 SOC concentration is consistent with the associated decrease in the $\delta^{13}\text{C}$ signature of SOM (Figure 3a), as
367 previously reported for glacier forelands in the Alps and Alaska (Bardgett et al., 2007; Guelland et al., 2013;
368 Malone et al., 2018). Increased SOC biogeochemical stability has been shown to be associated with an
369 increased $\delta^{13}\text{C}$ signature of SOM (Balesdent & Mariotti, 1996; Brüggemann et al., 2011; Menichetti et al.,
370 2015). However, we observed no correlation between $\delta^{13}\text{C}$ and soil age (Table 2), as previously reported
371 in an Alpine foreland (Smittenberg et al., 2012; but see Guelland et al., 2013, for contradictory results from
372 the same foreland). We infer that the stable carbon isotope signature of SOM is complex and does not
373 solely reflect its biogeochemical stability (Brüggemann et al., 2011).

374 The decrease in SOC stability with age and SOC concentration is also in line with previous observations of
375 a decrease in SOC thermal stability during the first 145 years of soil formation in a glacier foreland in the
376 European Alps (Bardgett et al., 2007). In contrast, Egli et al. (2010), who used a chemical fractionation
377 technique in their study, did not confirm this relationship. These inconsistencies are probably due to the
378 use of different methods. It should be noted, however, that chemical oxidation (*e.g.* hydrogen peroxide
379 treatment) is now not recommended to isolate the stable SOC kinetic pool (Lutfalla et al., 2014; Poeplau
380 et al., 2019). All SOM fractions isolated by physical, chemical or thermal methods are a mixture of labile
381 and stable carbon (Balesdent, 1996; von Lützow et al., 2007). In our study, the additional information on
382 thermal stability (Rock-Eval® T50 and T90 indexes) of the two main isolated thermal SOC fractions (Rock-
383 Eval® POC 2 and ROC) helped reducing biases inherent to SOM thermal fractionation methods. Indeed, the
384 slight increase in the proportion of the thermally stable ROC fraction (*ca.* +3.5 %; observed with soil age,
385 not with SOC concentration; Tables 2 and S2) does not mean that SOC accumulation is associated with an
386 increase in SOC biogeochemical stability, as evidenced by the consistent decrease in Rock-Eval® T50 and
387 T90 indexes observed with soil age and SOC concentration (Tables 2 and S2). This slight increase in the
388 proportion of the ROC fraction might be explained by the progressive accumulation of SOM of plant origin,
389 which is rich in cellulose and lignin, two compounds with a higher ROC fraction compared to other SOM
390 compounds such as lipids and proteins (Carrie et al., 2012). The increase in CH-POC 2 with soil age and SOC
391 concentration also highlights the accumulation of labile organic matter enriched in hydrogen moieties over
392 time (Barré et al., 2016; Gregorich et al., 2015; Poeplau et al., 2019; Saenger et al., 2015; Soucémariadin
393 et al., 2018). Finally, the consistent decrease in SOC stability with SOC accumulation in glacier forelands
394 supports the increasing body of evidence that SOC storage in most terrestrial ecosystem is driven by the
395 accumulation of labile SOC (see *e.g.* Barré et al., 2017, and references therein). This labile SOC is highly
396 vulnerable to global warming (Cotrufo et al., 2019; Viscarra Rossel et al., 2019).

397 Second, we detected a decreasing proportion of the thermally highly labile POC 1 fraction in the early
398 stages of soil formation (from ~3.2 % of total SOC, 9 to 50 years post deglaciation to ~1.3 % in the
399 oldest soils; Figures 4a, 5). In comparison, we have measured an average proportion of the POC 1 fraction
400 of 0.006% in fifty-one "mature" alpine grassland topsoils (0 to 5–10 cm) in the Grand Galibier massif in the
401 south-western French Alps (unpublished results). The high proportion of the labile SOC fraction in the
402 initial stages of new soils compared to "mature" ones has been previously reported and interpreted in
403 different ways. It might be due to a particularly high biomass of some soil microorganisms, such as
404 cyanobacteria (Schmidt et al., 2008), or to an important necromass consisting of dead cell-envelope
405 fragments from autotrophic or heterotrophic microbes (Bardgett et al., 2007; Schurig et al., 2013) that
406 could contribute to SOM during the initial stage of soil formation. It might also be due to the higher
407 proportion of an easily mineralizable SOC fraction, such as dissolved organic carbon produced within the
408 glacier (Guelland et al., 2013; Yoshitake et al., 2018), or to an easily mineralizable fraction of fossil organic
409 carbon (hydrogen-rich and thermally labile ; Copard et al., 2006 ; Graz et al., 2011). The decrease in the
410 index CH-POC 1 with soil age and with SOC concentration corresponds to a decrease in thermally labile
411 hydrogen-rich, and a relative increase in oxygen-rich, organic compounds with age in the POC 1 fraction.
412 The microbial biomass of some taxa (*e.g.* cyanobacteria) has been shown to be enriched in hydrogen
413 moieties (Carrie et al., 2012), thus the decrease in the CH-POC 1 index with soil age might reflect a temporal
414 decrease in the specific soil microbial biomass, or to the mineralization of the above-mentioned fraction
415 of fossil organic carbon (Copard et al., 2006 ; Graz et al., 2011). However, due to the limited chemical
416 information provided by Rock-Eval®, it is not possible to assess the exact chemical nature or origin of the
417 POC 1 thermally labile SOC pool.

418

419 **Origin of soil organic matter**

420 The C/N ratio and the relative composition of SOM in organic carbon functional groups provide
421 information on the origin of SOM, regarding the contribution of plant material and microorganisms. The
422 C/N ratio significantly increased with soil age (Figures 2c and 5), just as the SOM content in aromatic carbon
423 as previously shown by Egli et al., 2010) in the Swiss Alps (Table 2; Figure 5). A SOM C/N ratio of about 6,
424 observed in recently deglaciated topsoils, is characteristic of SOM of microbial origin (Paul and Clark,
425 1996) that can be recent or ancient (see *e.g.* Graz et al., 2011, for observed low C/N ratios of fossil SOM).
426 After 100 years of soil formation, the C/N ratio of SOM increased towards a value around 10 for certain
427 chronosequences, matching the typical C/N of surface soils (*e.g.* 11.6; Kirkby et al., 2011). At older sites,
428 the higher C/N ratio, the higher aromaticity (with FTIR C=C ratio approaching values typical from the
429 particulate organic matter fraction of topsoils; Soucémariadin et al., 2019), and the CH-POC 2 index of
430 SOM shows a transition towards a SOM largely derived from plants (Figure 5). This transition occurred
431 faster in glacier forelands in warm climates, where vegetation colonization and growth was more rapid
432 than in forelands in cold climates.

433 Stable isotopes of carbon and nitrogen can also provide useful, although not unambiguous, information
434 on the origin and cycling of the SOM (Brüggemann et al., 2011; Craine et al., 2015; Malone et al., 2018;
435 Whiticar, 1996). High values of $\delta^{13}\text{C}$ in glacier foreland soils are generally interpreted, when C4 plants are
436 absent, as the presence of ancient carbon that could come from relics of soils of previous interglacial
437 cycles, or cryoconites soot and dust that have been deposited on the glacier (Baccolo et al., 2017; Bajerski
438 & Wagner, 2013; Guelland et al., 2013; Sattin et al., 2009; Stubbins et al., 2012). High $\delta^{13}\text{C}$ values of SOC
439 and soil CO_2 effluxes have been correlated to low ^{14}C signals corresponding to ancient carbon in soils from
440 two glacier forelands in the Alps (Bardgett et al., 2007; Guelland et al., 2013). Our results showed a high
441 $\delta^{13}\text{C}$ signature, especially in young soils (Figures 3a and 5). Along with this ^{13}C enrichment, we note that
442 the thermal stability of the POC 2 and ROC fractions is higher in younger soils. Although ancient organic
443 carbon's Rock-Eval[®] signature is quite variable (containing both thermally labile and thermally stable

444 carbon), some studies have demonstrated the relevance of this analysis for detecting ancient organic
445 carbon (*e.g.* Copard et al., 2006; Vindušková et al., 2015). Therefore, our results suggest that a small (from
446 *ca.* 0.5 to 2 g C kg⁻¹; Figure 2a), ancient and highly stable SOC fraction is present in most of the young
447 proglacial soils that developed in the early stages of glacier retreat. The use of this SOM as a substrate for
448 a high microbial pool as proposed by Bardgett et al. (2007), is probable, but not strictly demonstrated here.
449 Finally, the significant decrease in $\delta^{13}\text{C}$ with increased SOC concentration (Figure 3a) is an additional
450 evidence that newly accumulated SOM is mostly of plant origin (C4 plants being absent from glacier
451 forelands ecosystems).

452 The relative depletion of ¹⁵N in SOM indicates that a significant proportion of nitrogen can come from
453 atmospheric deposition (Handley et al., 1999; Lehmann et al., 2004) or microbial fixation (Boddey et al.,
454 2000). Both mechanisms can coexist, but more negative values of the $\delta^{15}\text{N}$ signature were systematically
455 found in forelands from the northern hemisphere. Similarly, Smittenberg et al. (2012) observed
456 comparable highly negative $\delta^{15}\text{N}$ values (*i.e.* -4 ‰) in topsoils from a glacier foreland in the European Alps.
457 These observations are consistent with inorganic N deposition documented over large areas of Europe and
458 North America (Galloway et al., 2004; Holland et al., 1997), and support the hypothesis of a significant
459 nitrogen contribution from atmospheric depositions. This N deposition is probably progressively buffered
460 as soils age through the arrival of plant-derived nitrogen, including isotope fractionation during SOM
461 decomposition, which explains the $\delta^{15}\text{N}$ increase with time (Figures 3b and 5; Amundson et al., 2003;
462 Craine et al., 2015; Malone et al., 2018).

463
464 In conclusion, our results indicated highly consistent patterns of SOM build-up in glacial forelands at the
465 global scale. The rate of SOM accumulation in topsoils is enhanced by higher temperature during the
466 warmest quarter, suggesting that climate and time are key drivers of SOM build-up during the initial stages
467 of soil formation after glacier retreat. The increase in the C/N ratio in SOM with soil age at all sites

468 illustrates that SOC accumulation occurred in spite of a slower, yet significant N storage in topsoil.
469 Furthermore, a highly stable and possibly ancient SOC fraction can act as starting point for the initial SOM
470 build-up, providing a key source of energy for early soil food webs. Finally, the general decrease in SOC
471 biogeochemical stability and the general increase in SOM aromaticity indicate that SOM that is newly
472 accumulated in glacier forelands soils is mostly labile and of plant origin. This highlights the vulnerability
473 of SOC stocks from proglacial areas to global warming, and suggests that their maintenance in a warmer
474 world largely depends on increased soil carbon inputs from plants.

475

476 ***Acknowledgements***

477 We thank Florence Savignac for her help with the Rock-Eval® thermal analysis of soil samples and Florent
478 Arthaud for his help with the statistical analysis. This study was partially funded by the European Research
479 Council under the European Community Horizon 2020 Programme, Grant Agreement no. 772284
480 (IceCommunities), and by the Ville de Paris under the Emergence(s) Programme (SOCUTE project).

481 **References**

- 482 Abatzoglou, J. T., Dobrowski, S. Z., Parks, S. A., & Hegewisch, K. C. (2018). TerraClimate, a high-resolution
483 global dataset of monthly climate and climatic water balance from 1958–2015. *Scientific Data*,
484 5(1), 170-191. <https://doi.org/10.1038/sdata.2017.191>
- 485 Adams, J. M., & Faure, H. (1998). A new estimate of changing carbon storage on land since the last glacial
486 maximum, based on global land ecosystem reconstruction. *Global and Planetary Change*, 16-17,
487 3-24. [https://doi.org/10.1016/S0921-8181\(98\)00003-4](https://doi.org/10.1016/S0921-8181(98)00003-4)
- 488 Adams, J. M., Faure, H., Faure-Denard, L., McGlade, J. M., & Woodward, F. I. (1990). Increases in
489 terrestrial carbon storage from the Last Glacial Maximum to the present. *Nature*, 348(6303),
490 711-714. <https://doi.org/10.1038/348711a0>
- 491 Albrecht, W. A. (1938). *Loss of Soil Organic Matter and Its Restoration*. US Department of agriculture.
- 492 Amundson, R., Austin, A. T., Schuur, E. A. G., Yoo, K., Matzek, V., Kendall, C., Uebersax, A., Brenner, D., &
493 Baisden, W. T. (2003). Global patterns of the isotopic composition of soil and plant nitrogen :
494 GLOBAL SOIL AND PLANT N ISOTOPES. *Global Biogeochemical Cycles*, 17(1).
495 <https://doi.org/10.1029/2002GB001903>
- 496 Aniya, M., & Skvarca, P. (2012). Little Ice Age advances of Glaciar Perito Moreno, Hielo Patagónico Sur,
497 South America. *Bulletin of Glaciological Research*, 30, 1-8. <https://doi.org/10.5331/bgr.30.1>
- 498 Baccolo, G., Di Mauro, B., Massabò, D., Clemenza, M., Nastasi, M., Delmonte, B., Prata, M., Prati, P.,
499 Previtali, E., & Maggi, V. (2017). Cryoconite as a temporary sink for anthropogenic species stored
500 in glaciers. *Scientific Reports*, 7(1), 9623. <https://doi.org/10.1038/s41598-017-10220-5>
- 501 Bajerski, F., & Wagner, D. (2013). Bacterial succession in Antarctic soils of two glacier forefields on
502 Larsemann Hills, East Antarctica. *FEMS Microbiology Ecology*, 85(1), 128-142.
503 <https://doi.org/10.1111/1574-6941.12105>

- 504 Balesdent, J. (1996). The significance of organic separates to carbon dynamics and its modelling in some
505 cultivated soils. *European Journal of Soil Science*, 47(4), 485-493. <https://doi.org/10.1111/j.1365->
506 2389.1996.tb01848.x
- 507 Balesdent, J., & Mariotti, A. (1996). Measurement of soil organic matter turnover using ¹³C natural
508 abundance. *Mass spectrometry of soils.*, 83-111.
- 509 Bardgett, R. D., Richter, A., Bol, R., Garnett, M. H., Bäumler, R., Xu, X., Lopez-Capel, E., Manning, D. A. C.,
510 Hobbs, P. J., Hartley, I. R., & Wanek, W. (2007). Heterotrophic microbial communities use ancient
511 carbon following glacial retreat. *Biology Letters*, 3(5), 487-490.
512 <https://doi.org/10.1098/rsbl.2007.0242>
- 513 Barré, P., Angers, D. A., Basile-Doelsch, I., Bispo, A., Cécillon, L., Chenu, C., Chevallier, T., Derrien, D.,
514 Eglin, T. K., & Pellerin, S. (2017). Ideas and perspectives : Can we use the soil carbon saturation
515 deficit to quantitatively assess the soil carbon storage potential, or should we explore other
516 strategies? *Biogeosciences Discussions*, 1-12. <https://doi.org/10.5194/bg-2017-395>
- 517 Barré, P., Plante, A. F., Cécillon, L., Lutfalla, S., Baudin, F., Bernard, S., Christensen, B. T., Eglin, T.,
518 Fernandez, J. M., Houot, S., Kätterer, T., Le Guillou, C., Macdonald, A., van Oort, F., & Chenu, C.
519 (2016). The energetic and chemical signatures of persistent soil organic matter. *Biogeochemistry*,
520 130(1-2), 1-12. <https://doi.org/10.1007/s10533-016-0246-0>
- 521 Behar, F., Beaumont, V., & De B. Penteadó, H. L. (2001). Rock-Eval 6 Technology : Performances and
522 Developments. *Oil & Gas Science and Technology*, 56(2), 111-134.
523 <https://doi.org/10.2516/ogst:2001013>
- 524 Bockheim, J. G., Birkeland, P. W., & Bland, W. L. (2000). *Carbon storage and accumulation rates in alpine*
525 *soils : Evidence from Holocene chronosequences*. CRC Press.

- 526 Boddey, R. M., Peoples, M. B., Palmer, B., & Dart, P. J. (2000). Use of the ^{15}N natural abundance
527 technique to quantify biological nitrogen fixation by woody perennials. *Nutrient cycling in*
528 *agroecosystems*, 57(3), 235-270.
- 529 Brüggemann, N., Gessler, A., Kayler, Z., Keel, S. G., Badeck, F., Barthel, M., Boeckx, P., Buchmann, N.,
530 Brugnoli, E., Esperschütz, J., Gavrichkova, O., Ghashghaie, J., Gomez-Casanovas, N., Keitel, C.,
531 Knohl, A., Kuptz, D., Palacio, S., Salmon, Y., Uchida, Y., & Bahn, M. (2011). Carbon allocation and
532 carbon isotope fluxes in the plant-soil-atmosphere continuum : A review. *Biogeosciences*, 8(11),
533 3457-3489. <https://doi.org/10.5194/bg-8-3457-2011>
- 534 Burga, C. A., Krüsi, B., Egli, M., Wernli, M., Elsener, S., Ziefle, M., Fischer, T., & Mavris, C. (2010). Plant
535 succession and soil development on the foreland of the Morteratsch glacier (Pontresina,
536 Switzerland) : Straight forward or chaotic? *Flora - Morphology, Distribution, Functional Ecology*
537 *of Plants*, 205(9), 561-576. <https://doi.org/10.1016/j.flora.2009.10.001>
- 538 Burnham, K. P., Anderson, D. R., & Burnham, K. P. (2002). A practical information-theoretic approach.
539 *Model selection and multimodel inference, 2nd ed. Springer, New York, 2.*
- 540 Carrie, J., Sanei, H., & Stern, G. (2012). Standardisation of Rock–Eval pyrolysis for the analysis of recent
541 sediments and soils. *Organic Geochemistry*, 46, 38-53.
- 542 Cécillon, L., Baudin, F., Chenu, C., Houot, S., Jolivet, R., Kätterer, T., Lutfalla, S., Macdonald, A., van Oort,
543 F., Plante, A. F., Savignac, F., Soucémariadin, L. N., & Barré, P. (2018). A model based on Rock-
544 Eval thermal analysis to quantify the size of the centennially persistent organic carbon pool in
545 temperate soils. *Biogeosciences*, 15(9), 2835-2849. <https://doi.org/10.5194/bg-15-2835-2018>
- 546 Chapin, F. S., Walker, L. R., Fastie, C. L., & Sharman, L. C. (1994). Mechanisms of Primary Succession
547 Following Deglaciation at Glacier Bay, Alaska. *Ecological Monographs*, 64(2), 149-175.
548 <https://doi.org/10.2307/2937039>

- 549 Collet, M. (2010). Suivi spatio-temporel des calottes glaciaires de l'Antisana et du Cotopaxi (Équateur).
550 Analyse par télédétection dans un contexte de changement climatique. *Mémoire de Master 2*.
- 551 Conen, F., Yakutin, M. V., Zumbunn, T., & Leifeld, J. (2007). Organic carbon and microbial biomass in two
552 soil development chronosequences following glacial retreat. *European Journal of Soil Science*,
553 58(3), 758-762. <https://doi.org/10.1111/j.1365-2389.2006.00864.x>
- 554 Copard, Y., Di-Giovanni, C., Martaud, T., Albéric, P., & Olivier, J.-E. (2006). Using Rock-Eval 6 pyrolysis for
555 tracking fossil organic carbon in modern environments : Implications for the roles of erosion and
556 weathering. *Earth Surface Processes and Landforms*, 31(2), 135-153.
557 <https://doi.org/10.1002/esp.1319>
- 558 Cossart, É., Fort, M., Jomelli, V., & Grancher, D. (2006). Les variations glaciaires en Haute Durance
559 (Briançonnais, Hautes-Alpes) depuis la fin du XIXe siècle : Mise au point d'après les documents
560 d'archives et la lichénométrie. *Quaternaire*, vol. 17/1, 75-92.
561 <https://doi.org/10.4000/quaternaire.694>
- 562 Cotrufo, M. F., Ranalli, M. G., Haddix, M. L., Six, J., & Lugato, E. (2019). Soil carbon storage informed by
563 particulate and mineral-associated organic matter. *Nature Geoscience*, 12(12), 989-994.
564 <https://doi.org/10.1038/s41561-019-0484-6>
- 565 Craine, J. M., Brookshire, E. N. J., Cramer, M. D., Hasselquist, N. J., Koba, K., Marin-Spiotta, E., & Wang, L.
566 (2015). Ecological interpretations of nitrogen isotope ratios of terrestrial plants and soils. *Plant
567 and Soil*, 396(1-2), 1-26. <https://doi.org/10.1007/s11104-015-2542-1>
- 568 Darmody, R. G., Allen, C. E., & Thorn, C. E. (2005). Soil Topochronosequences at Storbreen, Jotunheimen,
569 Norway. *Soil Science Society of America Journal*, 69(4), 1275-1287.
570 <https://doi.org/10.2136/sssaj2004.0204>

- 571 Disnar, J. R., Guillet, B., Keravis, D., Di-Giovanni, C., & Sebag, D. (2003). Soil organic matter (SOM)
572 characterization by Rock-Eval pyrolysis : Scope and limitations. *Organic Geochemistry*, 34(3),
573 327-343. [https://doi.org/10.1016/S0146-6380\(02\)00239-5](https://doi.org/10.1016/S0146-6380(02)00239-5)
- 574 Dümig, A., Häusler, W., Steffens, M., & Kögel-Knabner, I. (2012). Clay fractions from a soil
575 chronosequence after glacier retreat reveal the initial evolution of organo–mineral associations.
576 *Geochimica et Cosmochimica Acta*, 85, 1-18. <https://doi.org/10.1016/j.gca.2012.01.046>
- 577 Dümig, A., Smittenberg, R., & Kögel-Knabner, I. (2011). Concurrent evolution of organic and mineral
578 components during initial soil development after retreat of the Damma glacier, Switzerland.
579 *Geoderma*, 163(1-2), 83-94. <https://doi.org/10.1016/j.geoderma.2011.04.006>
- 580 Eckmeier, E., Mavris, C., Krebs, R., Pichler, B., & Egli, M. (2013). Black carbon contributes to organic
581 matter in young soils in the Morteratsch proglacial area (Switzerland). *Biogeosciences*, 10(3),
582 1265-1274. <https://doi.org/10.5194/bg-10-1265-2013>
- 583 Egli, M., Fitze, P., & Mirabella, A. (2001). Weathering and evolution of soils formed on granitic, glacial
584 deposits : Results from chronosequences of Swiss alpine environments. *CATENA*, 45(1), 19-47.
585 [https://doi.org/10.1016/S0341-8162\(01\)00138-2](https://doi.org/10.1016/S0341-8162(01)00138-2)
- 586 Egli, M., Favilli, F., Krebs, R., Pichler, B., & Dahms, D. (2012). Soil organic carbon and nitrogen
587 accumulation rates in cold and alpine environments over 1Ma. *Geoderma*, 183-184, 109-123.
588 <https://doi.org/10.1016/j.geoderma.2012.03.017>
- 589 Egli, M., Mavris, C., Mirabella, A., & Giaccari, D. (2010). Soil organic matter formation along a
590 chronosequence in the Morteratsch proglacial area (Upper Engadine, Switzerland). *CATENA*,
591 82(2), 61-69. <https://doi.org/10.1016/j.catena.2010.05.001>
- 592 Eichel, J., Corenblit, D., & Dikau, R. (2016). Conditions for feedbacks between geomorphic and vegetation
593 dynamics on lateral moraine slopes : A biogeomorphic feedback window: CONDITIONS FOR

- 594 BIOGEOMORPHIC FEEDBACKS ON LATERAL MORaine SLOPES. *Earth Surface Processes and*
595 *Landforms*, 41(3), 406-419. <https://doi.org/10.1002/esp.3859>
- 596 Erktan, A. (2013). *Interactions entre composition fonctionnelle de communautés végétales et formation*
597 *des sols sans des lits de ravines en cours de restauration écologique* (Doctoral dissertation,
598 Grenoble).
- 599 Fischer, A., Fickert, T., Schwaizer, G., Patzelt, G., & Groß, G. (2019). Vegetation dynamics in Alpine glacier
600 forelands tackled from space. *Scientific Reports*, 9(1), 13918. [https://doi.org/10.1038/s41598-](https://doi.org/10.1038/s41598-019-50273-2)
601 [019-50273-2](https://doi.org/10.1038/s41598-019-50273-2)
- 602 Galloway, J. N., Dentener, F. J., Capone, D. G., Boyer, E. W., Howarth, R. W., Seitzinger, S. P., Asner, G. P.,
603 Cleveland, C. C., Green, P. A., Holland, E. A., Karl, D. M., Michaels, A. F., Porter, J. H., Townsend,
604 A. R., & Vosmarty, C. J. (2004). Nitrogen Cycles : Past, Present, and Future. *Biogeochemistry*,
605 70(2), 153-226. <https://doi.org/10.1007/s10533-004-0370-0>
- 606 Gardent, M., Rabatel, A., Dedieu, J.-P., & Deline, P. (2014). Multitemporal glacier inventory of the French
607 Alps from the late 1960s to the late 2000s. *Global and Planetary Change*, 120, 24-37.
608 <https://doi.org/10.1016/j.gloplacha.2014.05.004>
- 609 Göransson, H., Olde Venterink, H., & Bååth, E. (2011). Soil bacterial growth and nutrient limitation along
610 a chronosequence from a glacier forefield. *Soil Biology and Biochemistry*, 43(6), 1333-1340.
611 <https://doi.org/10.1016/j.soilbio.2011.03.006>
- 612 Graz, Y., Di-Giovanni, C., Copard, Y., Elie, M., Faure, P., Laggoun Defarge, F., Lévêque, J., Michels, R., &
613 Olivier, J. E. (2011). Occurrence of fossil organic matter in modern environments : Optical,
614 geochemical and isotopic evidence. *Applied Geochemistry*, 26(8), 1302-1314.
615 <https://doi.org/10.1016/j.apgeochem.2011.05.004>

- 616 Gregorich, E. G., Gillespie, A. W., Beare, M. H., Curtin, D., Sanei, H., & Yanni, S. F. (2015). Evaluating
617 biodegradability of soil organic matter by its thermal stability and chemical composition. *Soil*
618 *Biology and Biochemistry*, *91*, 182-191. <https://doi.org/10.1016/j.soilbio.2015.08.032>
- 619 Guelland, K., Hagedorn, F., Smittenberg, R. H., Göransson, H., Bernasconi, S. M., Hajdas, I., &
620 Kretzschmar, R. (2013). Evolution of carbon fluxes during initial soil formation along the forefield
621 of Damma glacier, Switzerland. *Biogeochemistry*, *113*(1-3), 545-561.
622 <https://doi.org/10.1007/s10533-012-9785-1>
- 623 Handley, L. L., Austin, A. T., Stewart, G. R., Robinson, D., Scrimgeour, C. M., Raven, J. A., Heaton, T. H. E.,
624 & Schmidt, S. (1999). The $\delta^{15}\text{N}$ natural abundance ($\delta^{15}\text{N}$) of ecosystem samples reflects
625 measures of water availability. *Functional Plant Biology*, *26*(2), 185.
626 <https://doi.org/10.1071/PP98146>
- 627 Harden, J. W., Mark, R. K., Sundquist, E. T., & Stallard, R. F. (1992). Dynamics of Soil Carbon During
628 Deglaciation of the Laurentide Ice Sheet. *Science*, *258*(5090), 1921-1924.
629 <https://doi.org/10.1126/science.258.5090.1921>
- 630 He, L., & Tang, Y. (2008). Soil development along primary succession sequences on moraines of
631 Hailuoguo Glacier, Gongga Mountain, Sichuan, China. *CATENA*, *72*(2), 259-269.
632 <https://doi.org/10.1016/j.catena.2007.05.010>
- 633 Hock, R., Rasul, G., Adler, C., Cáceres, B., Gruber, S., Hirabayashi, Y., Jackson, M., Kääb, A., Kang, S.,
634 Kutuzov, S., Milner, A., Molau, U., Morin, S., Orlove, B., & Steltzer, H. (2019). *IPCC Special*
635 *Report on the Ocean and Cryosphere in a Changing Climate_Chapter 2.pdf*.
- 636 Holland, E. A., Braswell, B. H., Lamarque, J.-F., Townsend, A., Sulzman, J., Müller, J.-F., Dentener, F.,
637 Brasseur, G., Levy, H., Penner, J. E., & Roelofs, G.-J. (1997). Variations in the predicted spatial
638 distribution of atmospheric nitrogen deposition and their impact on carbon uptake by terrestrial

- 639 ecosystems. *Journal of Geophysical Research: Atmospheres*, *102*(D13), 15849-15866.
640 <https://doi.org/10.1029/96JD03164>
- 641 Jobbágy, E. G., & Jackson, R. B. (2000). The vertical distribution of soil organic carbon and its relation to
642 climate and vegetation. *Ecological Applications*, *10*(2), 423-436. [https://doi.org/10.1890/1051-0761\(2000\)010\[0423:TVDOSO\]2.0.CO;2](https://doi.org/10.1890/1051-0761(2000)010[0423:TVDOSO]2.0.CO;2)
- 644 Johnson, E. A., & Miyanishi, K. (2008). Testing the assumptions of chronosequences in succession.
645 *Ecology Letters*, *11*(5), 419-431. <https://doi.org/10.1111/j.1461-0248.2008.01173.x>
- 646 Karger, D. N., Conrad, O., Böhrner, J., Kawohl, T., Kreft, H., Soria-Auza, R. W., Zimmermann, N. E., Linder,
647 H. P., & Kessler, M. (2017). Climatologies at high resolution for the earth's land surface areas.
648 *Scientific Data*, *4*(1), 170122. <https://doi.org/10.1038/sdata.2017.122>
- 649 Körner, C. (2003). *Alpine plant life : Functional plant ecology of high mountain ecosystems*. Springer
650 Science&Business Media.
- 651 Larocque, S. J., & Smith, D. J. (2003). Little Ice Age glacial activity in the Mt. Waddington area, British
652 Columbia Coast Mountains, Canada. *Canadian Journal of Earth Sciences*, *40*(10), 1413-1436.
653 <https://doi.org/10.1139/e03-053>
- 654 Lehmann, M. F., Bernasconi, S. M., McKenzie, J. A., Barbieri, A., Simona, M., & Veronesi, M. (2004).
655 Seasonal variation of the δC and δN of particulate and dissolved carbon and nitrogen in Lake
656 Lugano : Constraints on biogeochemical cycling in a eutrophic lake. *Limnology and
657 Oceanography*, *49*(2), 415-429. <https://doi.org/10.4319/lo.2004.49.2.0415>
- 658 Lutfalla, S., Chenu, C., & Barré, P. (2014). Are chemical oxidation methods relevant to isolate a soil pool
659 of centennial carbon? *Biogeochemistry*, *118*(1-3), 135-139. <https://doi.org/10.1007/s10533-013-9910-9>
660

- 661 Malone, E., Abbott, B., Klaar, M., Kidd, C., Sebiló, M., Milner, A., & Pinay, G. (2018). Decline in Ecosystem
662 $\delta^{13}\text{C}$ and Mid-Successional Nitrogen Loss in a Two-Century Postglacial Chronosequence.
663 *Ecosystems*, 21(8), 1659-1675.
- 664 Mavris, C., Egli, M., Plötze, M., Blum, J. D., Mirabella, A., Giaccari, D., & Haeberli, W. (2010). Initial stages
665 of weathering and soil formation in the Morteratsch proglacial area (Upper Engadine,
666 Switzerland). *Geoderma*, 155(3-4), 359-371. <https://doi.org/10.1016/j.geoderma.2009.12.019>
- 667 Medford, A. (2013). *Holocene Glacial History of Renland, East Greenland Reconstructed From Lake*
668 *Sediments*.
- 669 Menichetti, L., Houot, S., van Oort, F., Kätterer, T., Christensen, B. T., Chenu, C., Barré, P., Vasilyeva, N.
670 A., & Ekblad, A. (2015). Increase in soil stable carbon isotope ratio relates to loss of organic
671 carbon : Results from five long-term bare fallow experiments. *Oecologia*, 177(3), 811-821.
672 <https://doi.org/10.1007/s00442-014-3114-4>
- 673 Nakatsubo, T., Bekku, Y. S., Uchida, M., Muraoka, H., Kume, A., Ohtsuka, T., Masuzawa, T., Kanda, H., &
674 Koizumi, H. (2005). Ecosystem development and carbon cycle on a glacier foreland in the high
675 Arctic, Ny-Ålesund, Svalbard. *Journal of Plant Research*, 118(3), 173-179.
676 <https://doi.org/10.1007/s10265-005-0211-9>
- 677 Pelfini, M., Leonelli, G., Trombino, L., Zerboni, A., Bollati, I., Merlini, A., Smiraglia, C., & Diolaiuti, G.
678 (2014). New data on glacier fluctuations during the climatic transition at ~4,000 cal. Year BP from
679 a buried log in the Forni Glacier forefield (Italian Alps). *Rendiconti Lincei*, 25(4), 427-437.
680 <https://doi.org/10.1007/s12210-014-0346-5>
- 681 Pfeffer, W. T., Arendt, A. A., Bliss, A., Bolch, T., Cogley, J. G., Gardner, A. S., Hagen, J.-O., Hock, R., Kaser,
682 G., Kienholz, C., Miles, E. S., Moholdt, G., Mölg, N., Paul, F., Radić, V., Rastner, P., Raup, B. H.,
683 Rich, J., Sharp, M. J., & The Randolph Consortium. (2014). The Randolph Glacier Inventory : A

- 684 globally complete inventory of glaciers. *Journal of Glaciology*, 60(221), 537-552.
685 <https://doi.org/10.3189/2014JoG13J176>
- 686 Plante, A. F., Beaupré, S. R., Roberts, M. L., & Baisden, T. (2013). Distribution of Radiocarbon Ages in Soil
687 Organic Matter by Thermal Fractionation. *Radiocarbon*, 55(2), 1077-1083.
688 <https://doi.org/10.1017/S0033822200058215>
- 689 Poeplau, C., Barré, P., Cécillon, L., Baudin, F., & Sigurdsson, B. D. (2019). Changes in the Rock-Eval
690 signature of soil organic carbon upon extreme soil warming and chemical oxidation—A
691 comparison. *Geoderma*, 337, 181-190. <https://doi.org/10.1016/j.geoderma.2018.09.025>
- 692 Rabatel, A. (2005). *Chronologie et interprétation paléoclimatique des fluctuations des glaciers dans les*
693 *Andes de Bolivie (16 S) depuis le maximum du Petit Age Glaciaire (17ème siècle)* (Doctoral
694 dissertation).
- 695 Rabatel, A., Dedieu, J.-P., Thibert, E., Letréguilly, A., & Vincent, C. (2008). 25 years (1981–2005) of
696 equilibrium-line altitude and mass-balance reconstruction on Glacier Blanc, French Alps, using
697 remote-sensing methods and meteorological data. *Journal of Glaciology*, 54(185), 307-314.
698 <https://doi.org/10.3189/002214308784886063>
- 699 Rabatel, A., Jomelli, V., Naveau, P., Francou, B., & Grancher, D. (2005). Dating of Little Ice Age glacier
700 fluctuations in the tropical Andes : Charquini glaciers, Bolivia, 16°S. *Comptes Rendus Geoscience*,
701 337(15), 1311-1322. <https://doi.org/10.1016/j.crte.2005.07.009>
- 702 Richards, B. W. M., Benn, D. I., Owen, L. A., Rhodes, E. J., & Spencer, J. Q. (2000). Timing of late
703 Quaternary glaciations south of Mount Everest in the Khumbu Himal, Nepal. *Geological Society*
704 *of America Bulletin*, 12.
- 705 Rollinson, H. R. (1993). *Using geochemical data : Evaluation, presentation, interpretation*. Longman
706 Scientific & Technical ; Copublished in the U.S. with J. Wiley & Sons.

- 707 Saenger, A., Cécillon, L., Poulencard, J., Bureau, F., De Daniéli, S., Gonzalez, J.-M., & Brun, J.-J. (2015).
708 Surveying the carbon pools of mountain soils : A comparison of physical fractionation and Rock-
709 Eval pyrolysis. *Geoderma*, 241-242, 279-288. <https://doi.org/10.1016/j.geoderma.2014.12.001>
- 710 Sanderman, J., & Grandy, A. S. (2020). Ramped thermal analysis for isolating biologically meaningful soil
711 organic matter fractions with distinct residence times. *SOIL*, 6(1), 131-144.
712 <https://doi.org/10.5194/soil-6-131-2020>
- 713 Sattin, S. R., Cleveland, C. C., Hood, E., Reed, S. C., King, A. J., Schmidt, S. K., Robeson, M. S., Ascarrunz,
714 N., & Nemergut, D. R. (2009). Functional shifts in unvegetated, perhumid, recently-deglaciated
715 soils do not correlate with shifts in soil bacterial community composition. *The Journal of*
716 *Microbiology*, 47(6), 673-681. <https://doi.org/10.1007/s12275-009-0194-7>
- 717 Schielzeth, H., & Forstmeier, W. (2009). Conclusions beyond support : Overconfident estimates in mixed
718 models. *Behavioral Ecology*, 20(2), 416-420. <https://doi.org/10.1093/beheco/arn145>
- 719 Schlesinger, W. H. (1995). An overview of the carbon cycle. *Soils and global change*, 25, 9-25.
- 720 Schlesinger, W. H. (1990). Evidence from chronosequence studies for a low carbon-storage potential of
721 soils. *Nature*, 348(6298), 232-234. <https://doi.org/10.1038/348232a0>
- 722 Schmidt, S. K., Reed, S. C., Nemergut, D. R., Stuart Grandy, A., Cleveland, C. C., Weintraub, M. N., Hill, A.
723 W., Costello, E. K., Meyer, A. F., Neff, J. C., & Martin, A. M. (2008). The earliest stages of
724 ecosystem succession in high-elevation (5000 metres above sea level), recently deglaciated soils.
725 *Proceedings of the Royal Society B: Biological Sciences*, 275(1653), 2793-2802.
726 <https://doi.org/10.1098/rspb.2008.0808>
- 727 Schulz, S., Brankatschk, R., Dümig, A., Kögel-Knabner, I., Schloter, M., & Zeyer, J. (2013). The role of
728 microorganisms at different stages of ecosystem development for soil formation.
729 *Biogeosciences*, 10(6), 3983-3996. <https://doi.org/10.5194/bg-10-3983-2013>

- 730 Schurig, C., Smittenberg, R. H., Berger, J., Kraft, F., Woche, S. K., Goebel, M.-O., Heipieper, H. J., Miltner,
731 A., & Kaestner, M. (2013). Microbial cell-envelope fragments and the formation of soil organic
732 matter : A case study from a glacier forefield. *Biogeochemistry*, *113*(1-3), 595-612.
733 <https://doi.org/10.1007/s10533-012-9791-3>
- 734 Schweizer, S. A., Hoeschen, C., Schlüter, S., Kögel-Knabner, I., & Mueller, C. W. (2018). Rapid soil
735 formation after glacial retreat shaped by spatial patterns of organic matter accrual in
736 microaggregates. *Global Change Biology*, *24*(4), 1637-1650. <https://doi.org/10.1111/gcb.14014>
- 737 Smiraglia, C., & Azzoni, R. S. (2015). The New Italian Glacier Inventory : A didactic tool for a better
738 knowledge of the natural Alpine environment. *Rivista J-Reading n. 1-2015 - Journal of Research
739 and Didactics in Geography*. <https://doi.org/10.4458/5196-08>
- 740 Smith, J. U., Smith, P., Monaghan, R., & MacDonald, A. J. (2002). When is a measured soil organic matter
741 fraction equivalent to a model pool? *European Journal of Soil Science*, *53*(3), 405-416.
742 <https://doi.org/10.1046/j.1365-2389.2002.00458.x>
- 743 Smittenberg, R. H., Gierga, M., Göransson, H., Christl, I., Farinotti, D., & Bernasconi, S. M. (2012).
744 Climate-sensitive ecosystem carbon dynamics along the soil chronosequence of the Damma
745 glacier forefield, Switzerland. *Global Change Biology*, *18*(6), 1941-1955.
746 <https://doi.org/10.1111/j.1365-2486.2012.02654.x>
- 747 Soucémariadin, L., Cécillon, L., Chenu, C., Baudin, F., Nicolas, M., Girardin, C., & Barré, P. (2018). Is
748 Rock-Eval 6 thermal analysis a good indicator of soil organic carbon lability? – A method-
749 comparison study in forest soils. *Soil Biology and Biochemistry*, *117*, 108-116.
750 <https://doi.org/10.1016/j.soilbio.2017.10.025>
- 751 Soucémariadin, L., Cécillon, L., Chenu, C., Baudin, F., Nicolas, M., Girardin, C., Delahaie, A., & Barré, P.
752 (2019). Heterogeneity of the chemical composition and thermal stability of particulate organic

- 753 matter in French forest soils. *Geoderma*, 342, 65-74.
754 <https://doi.org/10.1016/j.geoderma.2019.02.008>
- 755 Stubbins, A., Hood, E., Raymond, P. A., Aiken, G. R., Sleighter, R. L., Hernes, P. J., Butman, D., Hatcher, P.
756 G., Striegl, R. G., Schuster, P., Abdulla, H. A. N., Vermilyea, A. W., Scott, D. T., & Spencer, R. G. M.
757 (2012). Anthropogenic aerosols as a source of ancient dissolved organic matter in glaciers.
758 *Nature Geoscience*, 5(3), 198-201. <https://doi.org/10.1038/ngeo1403>
- 759 Tielidze, L. G., Kumladze, R. M., Wheate, R. D., & Gamkrelidze, M. (2019). The Devdoraki Glacier
760 Catastrophes, Georgian Caucasus. *Hungarian Geographical Bulletin*, 21-35.
761 <https://doi.org/10.15201/hungeobull.68.1.2>
- 762 Vindušková, O., Sebag, D., Cailleau, G., Brus, J., & Frouz, J. (2015). Methodological comparison for
763 quantitative analysis of fossil and recently derived carbon in mine soils with high content of
764 aliphatic kerogen. *Organic Geochemistry*, 89-90, 14-22.
765 <https://doi.org/10.1016/j.orggeochem.2015.10.001>
- 766 Viscarra Rossel, R. A., Lee, J., Behrens, T., Luo, Z., Baldock, J., & Richards, A. (2019). Continental-scale soil
767 carbon composition and vulnerability modulated by regional environmental controls. *Nature*
768 *Geoscience*, 12(7), 547-552. <https://doi.org/10.1038/s41561-019-0373-z>
- 769 von Lützw, M., Kögel-Knabner, I., Ekschmitt, K., Flessa, H., Guggenberger, G., Matzner, E., & Marschner,
770 B. (2007). SOM fractionation methods : Relevance to functional pools and to stabilization
771 mechanisms. *Soil Biology and Biochemistry*, 39(9), 2183-2207.
772 <https://doi.org/10.1016/j.soilbio.2007.03.007>
- 773 Walker, L. R., Wardle, D. A., Bardgett, R. D., & Clarkson, B. D. (2010). The use of chronosequences in
774 studies of ecological succession and soil development : Chronosequences, succession and soil
775 development. *Journal of Ecology*, 98(4), 725-736. [https://doi.org/10.1111/j.1365-](https://doi.org/10.1111/j.1365-2745.2010.01664.x)
776 [2745.2010.01664.x](https://doi.org/10.1111/j.1365-2745.2010.01664.x)

- 777 Whiticar, M. J. (1996). Stable isotope geochemistry of coals, humic kerogens and related natural gases.
778 *International Journal of Coal Geology*, 32(1-4), 191-215. <https://doi.org/10.1016/S0166->
779 5162(96)00042-0
- 780 Wietrzyk, P., Rola, K., Osyczka, P., Nicia, P., Szymański, W., & Węgrzyn, M. (2018). The relationships
781 between soil chemical properties and vegetation succession in the aspect of changes of distance
782 from the glacier forehead and time elapsed after glacier retreat in the Irenebreen foreland (NW
783 Svalbard). *Plant and Soil*, 428(1-2), 195-211. <https://doi.org/10.1007/s11104-018-3660-3>
- 784 Yoshitake, S., Uchida, M., Imura, Y., Ohtsuka, T., & Nakatsubo, T. (2018). Soil microbial succession along
785 a chronosequence on a High Arctic glacier foreland, Ny-Ålesund, Svalbard : 10 years' change.
786 *Polar Science*, 16, 59-67. <https://doi.org/10.1016/j.polar.2018.03.003>
787
788

789 Table 1. Glacier forelands sampled and bibliographic sources used to date moraines.

Name	Mountain region	Country	Lat. (° E)	Long. (° N)	Elevation of glacier front (m a.s.l.)	Elevation of oldest sample site (m a.s.l.)	Lithology	Studied time period since deglaciation (years) and number of study sites	Data sources for soil chronology
Apusnikajik	Renland	Greenland	71.26	-25.82	75	55	Granite and gneiss	10-150; n = 3	Medford, 2013
Perito Moreno	South Andes	Argentina	-50.5	-73.04	180	340	Granite and granodiorite	100-410; n = 3	Aniya & Skvarca, 2012
Tiedemann	North Pacific Range	Canada	51.32	-124.923	950	815	Granodiorite and orthogneiss	36-116; n = 3	Larocque & Smith, 2003
Forni	Central European Alps	Italy	46.41	10.57	2600	2200	Granite	10-150; n = 7	Pelfini et al., 2014
Glaciers Noir/Blanc	Western European Alps	France	44.92	6.41	2670	1890	Granite	14-166; n = 8	Cossart et al., 2006; Rabatel et al., 2008
Gergeti	Greater Caucasus	Georgia	42.66	44.55	3220	2770	Andesite and dacite	15-150; n = 5	Tielidze et al., 2019
Lobuche	Central Himalaya	Nepal	27.96	86.81	5100	5020	Black gneiss, metapelite and quartzite	20-300; n = 5	Richards et al., 2000
Charquini	Central Andes	Bolivia	-16.31	-68.11	5070	4830	Granodiorite and granite	9-350; n = 7	Rabatel et al., 2005
Zongo	Central Andes	Bolivia	-16.27	-68.13	4940	4830	Granite	9-351; n = 7	Rabatel, 2005
Antisana	Northern Andes	Ecuador	-0.47	-78.15	4870	4780	Andesite and volcanic ash	17-150; n = 5	Collet, 2010

790

791

792 Table 2. Results of general mixed models that assess relationships between the SOM characteristics and
 793 soil age, mean temperature of warmest quarter (T) and precipitation of warmest quarter (P). Two types of
 794 mixed models were tested: models with random intercept (RI) and random slope (RS). The table includes
 795 results only for the mixed models with the lowest AICs values. Symbols for p values: *** $p < 0.001$; ** $p <$
 796 0.01 ; * $p < 0.05$; † $p < 0.1$; NS > 0.1 . In brackets are the B values, indicating the direction of the relationships.
 797 Other models tested and detailed results are presented in Tables S1 and S3.

	Model	Soil age	T	P	Age:T	Age:P	R ²
SOC (g C kg ⁻¹)	RS	*** (0.85)	* (0.70)		* (0.26)		0.51
Ntot (g N kg ⁻¹)	RI	*** (0.66)	† (0.47)		** (0.27)	† (0.14)	0.41
C/N	RI	*** (2.39)	* (1.88)		† (0.56)	† (-0.46)	0.54
δ ¹³ C (‰)	RS		** (-0.82)				0.20
δ ¹⁵ N (‰)	RI	** (0.71)	* (-0.82)		† (0.49)		0.26
POC 1 (g C kg ⁻¹)	RI	** (0.32)	* (0.38)	* (0.37)			0.36
POC 2 (g C kg ⁻¹)	RI	*** (0.90)	* (0.67)	* (0.64)	* (0.43)	† (0.41)	0.57
ROC (g C kg ⁻¹)	RI	*** (0.95)	* (0.68)	* (0.60)	* (0.45)	NS	0.62
POC 1 (% of total SOC)	RI	*** (-0.48)	† (-0.31)	* (-0.35)			0.50
POC 2 (% of total SOC)	RI	† (-0.06)				* (0.09)	0.17
ROC (% of total SOC)	RI	*** (0.13)	† (0.05)			** (-0.10)	0.38
T50-POC 2 (°C)	RI	*** (-0.03)					0.33
T50-ROC (°C)	RI	*** (-0.02)					0.08
CH-POC 1	RI	*** (-0.39)	NS		* (-0.37)	NS	0.30
CH-POC 2	RI	* (0.18)		† (0.13)	* (0.29)	** (0.36)	0.38
FTIR C=C	RS	** (0.04)	* (0.02)		* (0.03)		0.36
FTIR C=O	RS	* (-0.02)	† (0.02)		* (-0.01)		0.29
FTIR C-H	RI	*** (-0.02)			** (-0.02)		0.29

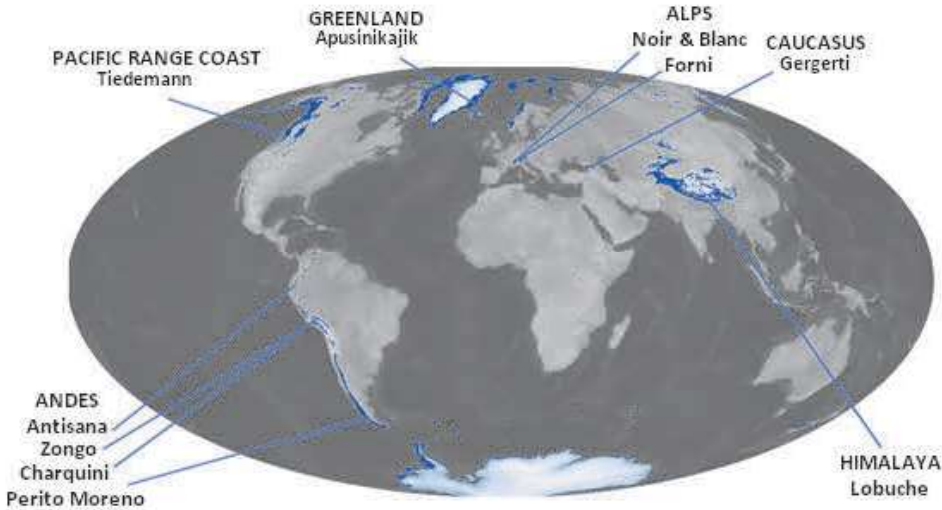


Figure 1. Locations of the ten glacier forelands of this study. Background map is modified from Randolph Glacier Inventory under an Attribution 4.0 International license (RGI Consortium, 2017).

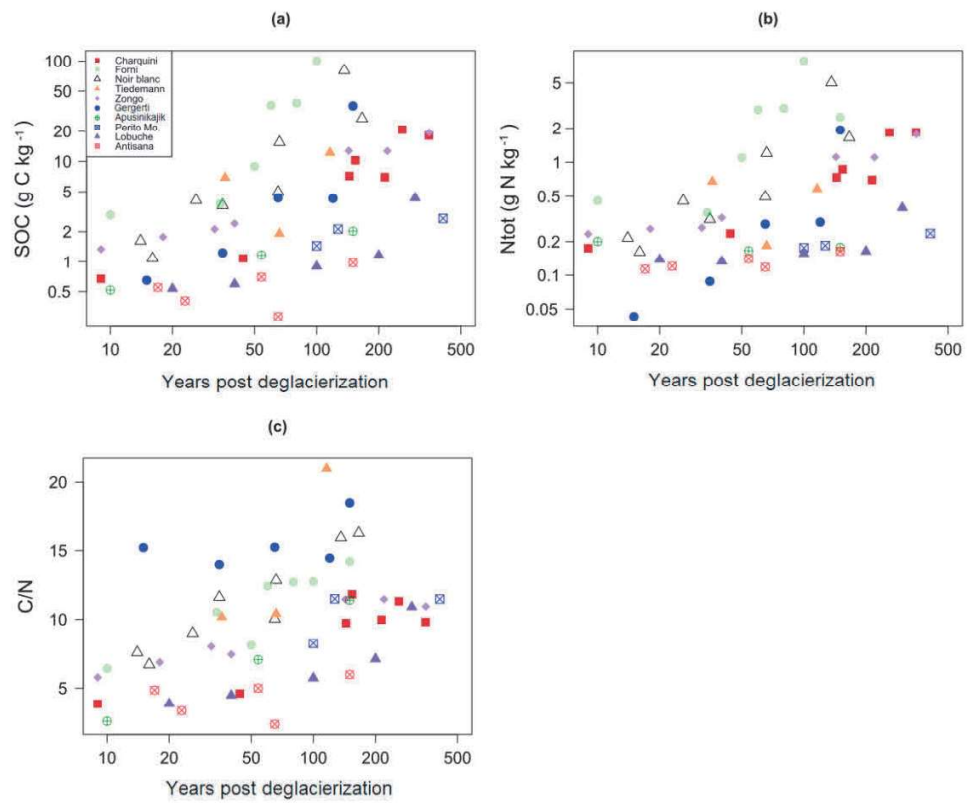


Figure 2. Plots of (a) SOC concentration, (b) total N (Ntot) concentration, and (c) C/N ratio of topsoil samples versus time for the ten soil chronosequences.

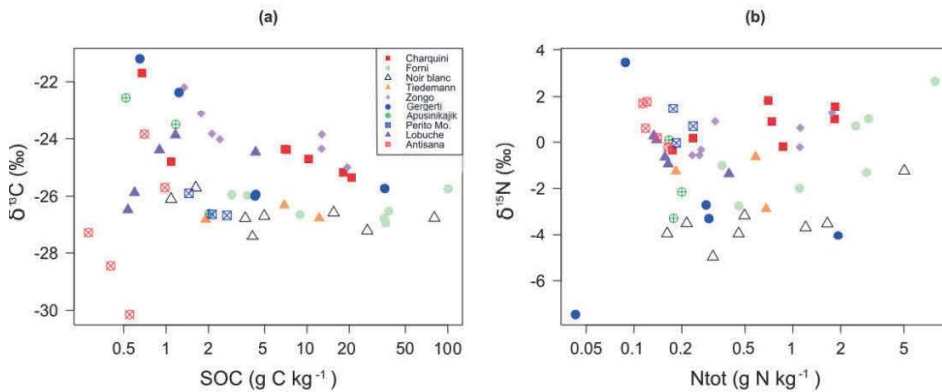


Figure 3. Plots of (a) soil $\delta^{13}\text{C}$ versus SOC, and (b) soil $\delta^{15}\text{N}$ evolution versus Ntot.

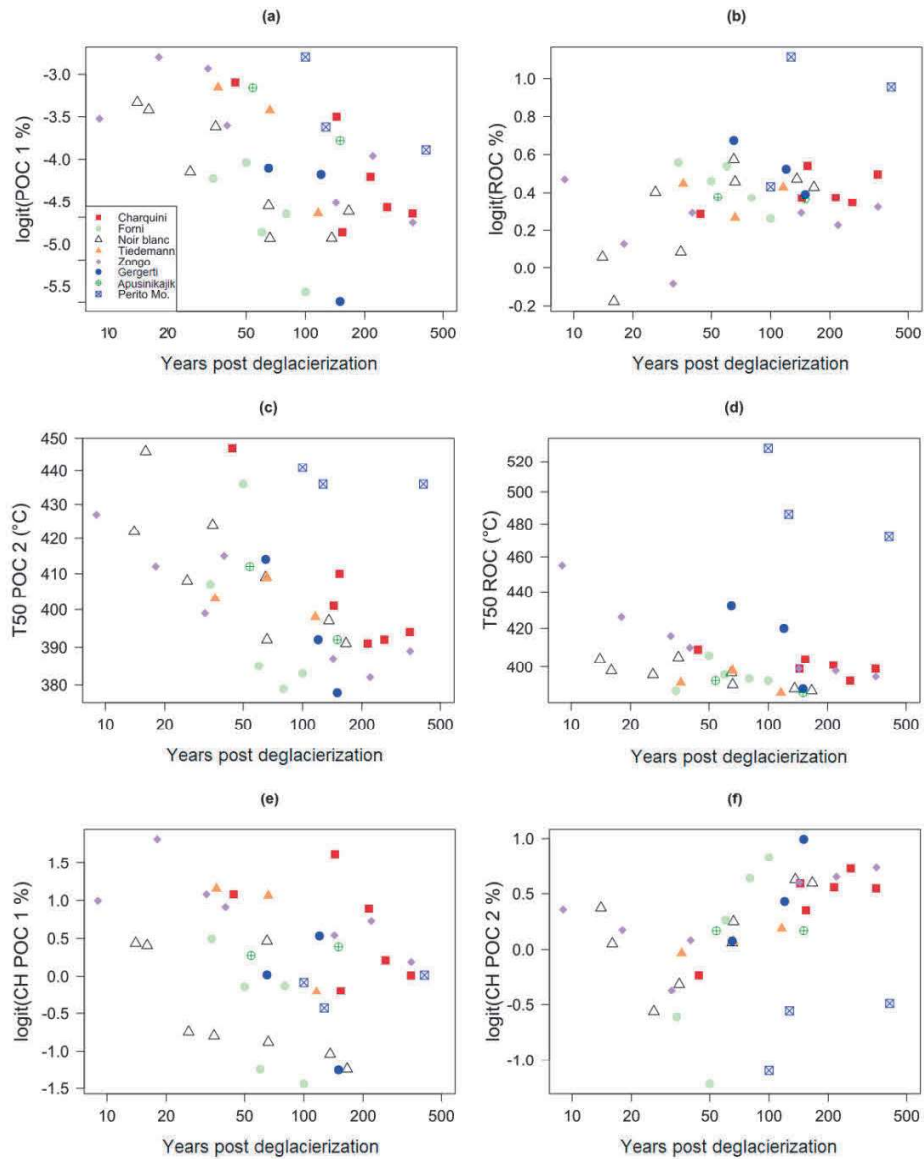


Figure 4. Relationships between soil age and (a) Rock-Eval® POC 1 (% of total SOC), (b) Rock-Eval® ROC (% of total SOC), (c) T50-POC 2, (d) T50-ROC, (e) CH-POC 1 index, and (f) CH-POC 2 index for eight proglacial soil chronosequences.

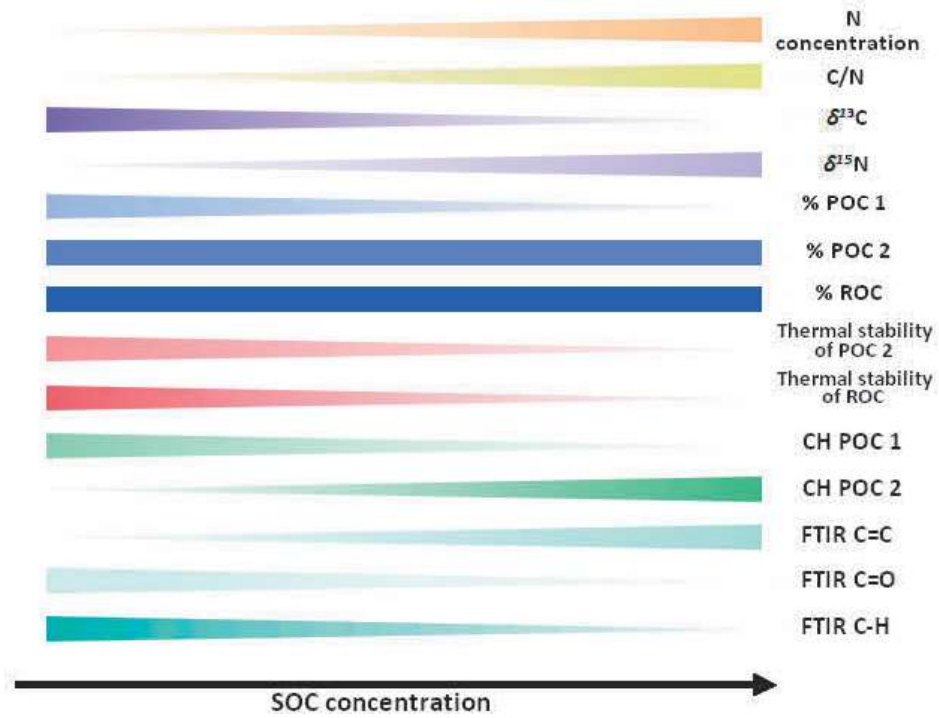


Figure 5. Overall trends in the biogeochemical signatures of soil organic matter (SOM) during its accumulation in recently deglaciated (up to four centuries) topsoils.